

The Cryosat land ice validation experiment 2004

Part II: Ground-based measurements of the firn structure using GPR

Thorben Dunse*, Veit Helm, Olaf Eisen, Daniel Steinhage, Wolfgang Rack

*University of Bremen, Department of Geosciences
 Alfred Wegener Institute for Polar and Marine Research
 email: tdunse@awi-bremerhaven.de



A Background

During CryoVex 2004, one of ESA's CryoSat validation campaigns, high resolution ground-penetrating radar measurements (GPR) were performed in the western part of the Greenland Ice Sheet. Principal objective of all CryoSat land ice validation activities is to assess and quantify uncertainty in the CryoSat measurements and to investigate the interaction of its radar altimeter with the upper meters of the snowpack.

The GPR data presented here, consists of lines of a detailed grid net

located at point T05 (70° N, 47° W) of the EGIG-line at an altitude of 1940m NN (Fig. 1 a & b), corresponding to the upper percolation zone. In this region surface melting occurs during the summer and melt water percolates into the snow pack where it refreezes and forms ice lenses or continuous layers of high density. Reflections of the radar pulse are attributed to changes of the dielectric constant, which - in dry snow and firn - is controlled by the density contrast (Tiuri et al., 1984).

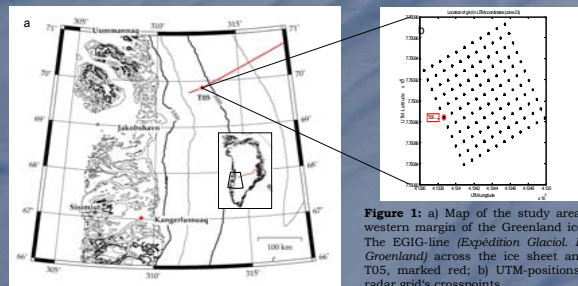


Figure 1: a) Map of the study area in the western margin of the Greenland ice sheet. The EGIG-line (*Expedition Glacial, Internat. Greenland*) across the ice sheet and point T05, marked red; b) UTM-positions of the radar grid's crosspoints

C Traveltime - Depth Conversion

The lefthand plot of Fig. 3 shows the permittivity profile ϵ' , derived from the firn-core data using Kovacs' empirical formula $\epsilon' = (1 + 0.845\rho_p)^2$ (1) where ρ_p the specific density and from which the electromagnetic wave speed v in the snow can be calculated (negligible liquid water content):

$$v = \frac{c}{\sqrt{\epsilon'}} \quad (2)$$

where c is the speed of light in vacuum. A permittivity value of 3.17 corresponds to pure ice (high freq. limit), while 1 would be air.

The blue line in the centre plot shows the traveltime-depth relation based on the core data, dashed lines are upper and lower limits for air and pure ice, respectively. Because the firn core was not drilled exactly on the GPR-profile, no attempt was made so far to correlate permittivity peaks with radar reflections.

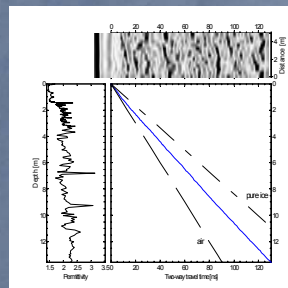


Figure 3: Left-hand plot: Snow-density based permittivity profile. Centre plot: Depth vs traveltime relation calculated using equation (1) and (2) for density data, air and pure ice. Upper plot: A 5 m wide strip of a 500 MHz radargram for possible correlation (Kohler et al., 1997).

B Data Sets & Methods

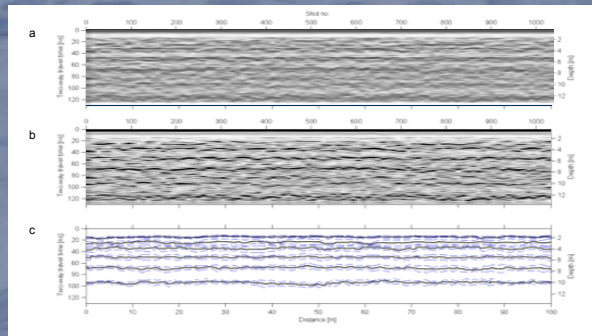


Figure 2: Amplitude (a) and envelope display (b) of filtered and gain corrected radar data, recorded with shielded 500 MHz antennae. c) digitized bands (dashed blue lines) and computed centreline (solid black line). Note, that horizons do not represent a complete set of progressive summer surfaces. Due to a high degree of discontinuity, not all events visible in the radargrams had been tracked.

Ground-penetrating radar

The GPR-data were collected using a commercial RAMAC radar system (Mala Geo-Science), operating with shielded antennae at frequencies of 500 and 800 MHz. The radar system and a GPS receiver for simultaneous position measurements were mounted on a man-pulled sledge (see top left pic.). The profiles form a grid of 100 x 100 m with 10 m line spacing.

Processing of the radar data includes individual correction of first arrival times, bandpass filtering, calculation of the envelope, smoothing and automatic gain control. With the amplitude being displayed, possible horizons appear rather as dark bands of high reflectivity, than as well defined reflectors (Fig. 2a). These bands become more focused, when the envelope is displayed (Fig. 2b).

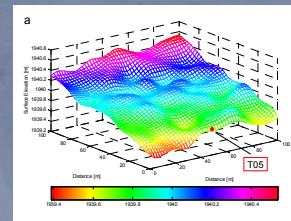
The upper and lower edges of each band had been digitized, followed by a computation of the centreline (Fig. 2c). This method takes into account the high ambiguity and discontinuity of most of the reflectors and provides additional information for interpretation, e.g. statistical analyses of the band width, as a measure of how well a reflector is defined.

Snow-pit & firn-core data

A density profile, derived from several snow pits and shallow cores (down to ~ 3 m depth) and one longer firn core (18.9 m), forms the bases in the conversion of travel time to depth (Eisen et al., 2002; see more below). Integration of the density field yields cumulative mass as a function of depth.

D Surface Topography & Internal Reflection Horizons

The surface elevation at the grid slightly increases eastwards, towards the summit of the ice sheet and ranges from 1939.2 to 1940.6 m. The surface topography is characterized by winddriven sastrugi.



Several internal horizons down to a depth of about 10m, including the last summer surface (lss), could be identified and tracked throughout the grid. The average depth of the lss is 1.84 m, corresponding to a cumulative mass of 571 kg/m². This value is larger than the annual mean accumulation rate of 470 kg/m²a water equivalent at T05, earlier reported (Fischer et al., 1995), but consistent with observations from the field parties and first results from a cross-over flight using the ASIRAS-system (Airborne SAR Interferometric Radar Altimeter System). No dating is available for the other horizons. With the above mean, the cumulative mass of 6972 kg/m² over the radar depth range of 13.5 m (129 ns) corresponds to 14.8 years of snow accumulation.

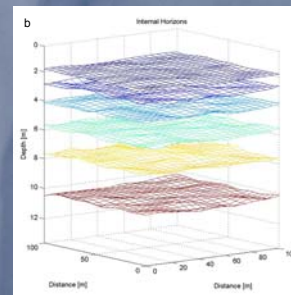


Figure 4: a) Surface Elevation of the grid; b) Internal reflection horizons relative to the surface, identified and tracked throughout the grid of 100 x 100 m. The time window of the radar was limited to 129 ns corresponding to a depth of ~13.5 m.

E Spatial Variation

Over the grid's scale of 100 x 100 m, internal reflection horizons appear to be almost parallel and show only minor variations in the order of decimeters, as the surface topography.

Fig. 5 displays histograms of the depth (a) and band width (b) of the lss. The mean depth is 1.84 m, with a standard deviation of 0.12 m (~68.3% of the data within that range). The mean band width is 0.485 ± 0.14 m.

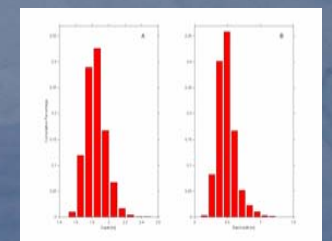


Figure 5: Histograms of the depth (A) and band width (B) of the last summer surface.

Acknowledgements

We acknowledge the performance of the field parties collecting the data, and thank Victoria Parry and Pete Nienow, Institute of Geography at the University of Edinburgh for supplying GPS, snow pit and firn-core records.

References

- Eisen, O. and Nixdorf, U. and Wilhelms, F. and Miller, H. (2002) Electromagnetic wave speed in polar ice: validation of the common-midpoint technique with high resolution dielectric-profiling and γ -density measurements. *Ann. Glac.* 34, 150-156.
- Fischer, H. and Wagenbach, D. and Latenser, M. and Haeblerl, W. (1995) Glacio-meteorological and isotopic studies along the EGIG line, central Greenland. *J. Glaciol.* 41, 515-527
- Kohler, J. and Moore, J. and Kennett, M. and Engeset, R. and Elvehoj, H. (1997) Using ground-penetrating radar to image previous years' summer surfaces for mass-balance measurements. *Ann. Glac.* 24, 355-360
- Kovacs, A. and Gow, A.J. and R.M. Morey (1985). The in-situ dielectric constant of polar firn revisited. *Cold Reg. Sci. & Technol.* 23, 245-256.
- Tiuri, M.E. and Sihvola, A.H. and Nyfors, E.G. and Hallikainen, M.T. (1984). The complex dielectric constant of snow at microwave frequencies. *J. Oceanogr. Eng.* 9, 377-382.